Journal of Electroanalytical Chemistry 724 (2014) 15–20

Contents lists available at ScienceDirect

Journal of Electroanalytical Chemistry

journal homepage: www.elsevier.com/locate/jelechem

Microscopic surface structures and ORR activities for vacuum-deposited Pt/Ni/Pt(1 1 1) and Pt/Ni/Pt(1 1 0) sandwich structures

N. Todoroki *, T. Dasai, Y. Asakimori, T. Wadayama

Graduate School of Environmental Studies, Tohoku University, Aoba-ku, Aramaki Aoba 6-6-2, Sendai 980-8579, Japan

ARTICLE INFO

Article history:
Received 4 March 2014
Received in revised form 10 April 2014
Accepted 11 April 2014
Available online 20 April 2014

Keywords:
Oxygen reduction reaction
Polymer electrolyte membrane fuel cell
Platinum-based alloys
Scanning tunneling microscopy
Low-energy electron diffraction
Molecular beam epitaxy

ABSTRACT

$Pt_{0.3–0.6nm}/Ni_{0.3–0.6nm}/Pt(1\,1\,1)$ and $Pt_{0.3–0.6nm}/Ni_{0.3–0.6nm}/Pt(1\,1\,0)$ atomic sandwich structures were prepared through alternating vacuum depositions of Ni followed by Pt onto clean Pt(1 1 1) and (1 1 0) substrates at room temperature under ultra-high-vacuum (UHV) conditions. After the samples were transferred from UHV to a 1-atm N_2 atmosphere, their oxygen reduction reaction (ORR) activities were evaluated in O_2-saturated 0.1 M $HClO_4$ at 0.9 V vs. reversible hydrogen electrode. $Pt_{0.6nm}/Ni_{0.6nm}/Pt(1\,1\,1)$ and $Pt_{0.6nm}/Ni_{0.6nm}/Pt(1\,1\,0)$ were most active among the respective Pt/Ni/Pt(1 1 1) and Pt/Ni/Pt(1 1 0) sandwich series: the activities of the former and latter sandwich structures were approximately five- and threefold greater than those of the corresponding clean Pt(1 1 1) and (1 1 0) substrate surfaces. Scanning tunneling microscopy images of the as-prepared $Pt_{0.6nm}/Ni_{0.6nm}/Pt(1\,1\,1)$ and $Pt_{0.6nm}/Ni_{0.6nm}/Pt(1\,1\,0)$ surfaces revealed three-dimensionally grown hexagonal-shaped small domains of Pt(1 1 1) (approximately 2 nm in size) and parallelogram-shape (1 1 0) terrace islands oriented along ⟨1 1 0⟩, respectively. The results indicate that not only the atomic arrangements of the topmost Pt layers but also the nanoscale morphologies of Pt–Ni in the surface vicinities determine the enhancement of the ORR activity of Pt–M alloy catalysts.

1. Introduction

Watanabe and co-workers first reported that Pt–M alloys (where M is an inexpensive metal such as Fe, Ni, and Co) exhibit greatly enhanced electrochemical (EC) oxygen reduction reaction (ORR) activities [1]. Since then, numerous studies of Pt–M nanoparticles (NPs) have been conducted to develop highly efficient electrode materials for use in polymer electrolyte membrane fuel cells (PEMFCs). Through these studies, a broad consensus has been reached that practical Pt–M catalysts, i.e., the synthesis of Pt–M alloys with Pt-enriched topmost surface structures (so-called Pt-skins), are a common target for the development of highly active and durable catalysts [2–5]. Active studies of Pt-shell and M-core core–shell NPs [6–8], the selective EC de-alloying of the M components of Pt–M NPs [9–12], and the fabrication of nanostructured thin films of Pt–M [13,14] and shape-controlled Pt–M NPs [15–18] are currently underway.

The mechanisms by which Pt–M alloys exhibit enhanced ORR activity have been widely discussed [19–25]. For example, the "*d*-band model" proposed by Hammer and Nørskov [26] successfully explains the trend in the activity enhancement with alloying elements. The authors demonstrated how 3*d* metals modify the electronic and chemical properties of a Pt surface via the ligand effect. However, the detailed mechanism of Pt–M catalysts are rather complicated because their ORR activities are highly sensitive to both the electronic properties of the surface Pt shell layers modified with underlaid M metals and the topmost surface morphologies of the surface Pt atoms. Atomic arrangements and compositions of bimetallic alloy surfaces are expected to seriously influence their electrocatalytic performance. Furthermore, the sizes of NPs [27–29] and the surface crystal plane orientations [19,30–33] of pure Pt are critical factors for the ORR enhancements.

Well-defined surface science approaches are fruitful for achieving a comprehensive understanding of the correlation between the ORR enhancements and the alloy surface and/or interface structures [34–36]. For example, Stamenkovic et al. evaluated the ORR activities of the (1 1 1), (1 0 0), and (1 1 0) single-crystal planes of an as-prepared Pt_3Ni alloy [37] and demonstrated that the activities were remarkably dependent on the surface crystallographic arrangements. Furthermore, Adzic and coworkers observed a trend in the ORR activities of electrochemically prepared Pt-monolayers on Pd(1 1 1), Au(1 1 1), Rh(1 1 1), Ir(1 1 1), and Ru(0 0 0 1) single-crystal surfaces [38]. Such well-defined approaches enable us to discuss the atomically flat, long-range periodical, topmost surfaces

* Corresponding author. Tel.: +81 227957320.
E-mail address: n-todoroki@material.tohoku.ac.jp (N. Todoroki).

http://dx.doi.org/10.1016/j.jelechem.2014.04.008
1572-6657/

of Pt–M alloys. In addition, the EC responses of the atomically flat, well-defined Pt–M surfaces under specific conditions should provide an essential clue to enable us to elucidate the ORR mechanisms of Pt–M catalysts and thereby directly link their properties to the development of practical Pt–M catalysts for PEMFCs. As an example, potential sweeps up to the standard electrode potentials of the less-noble metal M and potential cycling across the standard electrode potentials of M atomically modify the topmost bimetallic surface structures and thereby provide information related to the durability of Pt–M catalysts. From these viewpoints, we have effectively used molecular beam epitaxy (MBE) and ultra-high-vacuum (UHV) techniques to prepare model electrocatalyst surfaces for ORR and have investigated the initial ORR activities of the prepared bimetallic surfaces of Ni/Pt(1 1 1) [39–42], Co/Pt(h k l) [43], and Pt/Au(hkl) [44], and their ORR responses under specific EC conditions.

In this study, we focused on the ORR activities of Pt/Ni/Pt atomic sandwich structures prepared through the alternating vacuum depositions of Ni and Pt onto single-crystal Pt(1 1 1) and (1 1 0) substrates under UHV conditions. Although the fabricated Pt/Ni/Pt atomic sandwich structures are atomically rough relative to a clean Pt substrate or thermally grown, Pt-enriched, Pt–M single-crystal surfaces [42], the sandwich structures are considered to be a surface model for bridging the gap between the results obtained for practical alloy catalysts and those obtained for atomically flat, well-defined model surfaces.

2. Experimental

Pt/Ni/Pt(1 1 1) and Pt/Ni/Pt(1 1 0) atomic sandwich structures were prepared through alternate depositions of Ni followed by Pt onto clean Pt(1 1 1) and (1 1 0) substrate surfaces at room temperature. We used the UHV system (with a base pressure of 2×10^{-8} Pa) equipped with various surface science evaluation apparatus, including a scanning tunneling microscope (STM; JEOL 4500), a low-energy electron diffractometer (LEED; OCI BDL600), an X-ray gun (SPECS XR-50), and a hemi-cylindrical electron energy analyzer (SPECS PHOIBOS 1500) for X-ray photoelectron spectroscopy (XPS). The Pt(1 1 1) and (1 1 0) single-crystal substrates with less than 0.1° miscut (φ = 8 mm) were cleaned by being repeatedly sputtered with Ar^+ ions (PSP ISIS3000) and annealed at 1073 K under UHV. After the surface cleaning procedure, Ni and Pt (99.99% pure) were deposited onto the cleaned Pt single-crystal substrates using electron beam evaporators (Beamtron); the pressure during the depositions of Ni and Pt was less than 1×10^{-7} Pa. The deposition rates for both Pt and Ni were fixed at 0.1 and 0.05 nm/min, respectively, and were estimated using flux monitors installed in each evaporator that ware calibrated separately using a quartz microbalance. Given the atomic radii of Ni and Pt, the deposition thicknesses of 0.3 and 0.6 nm should correspond to approximately 1 and 2 monolayers, respectively. In this study, we denote the sandwich structures prepared through, for example, the deposition of 0.3-nm-thick Ni followed by the deposition of 0.3-nm-thick Pt onto Pt(1 1 1) as $Pt_{1ML}/Ni_{1ML}/Pt(1\,1\,1)$. The resulting Pt/Ni/Pt atomic sandwich surfaces were subsequently characterized by STM observations and LEED measurements.

The UHV-EC sample transfer system and the EC setup used in this study have been described elsewhere [40]. Briefly, the UHV-prepared Pt/Ni/Pt atomic sandwich structures were transferred from UHV into a N_2-purged stainless-steel glove box without air exposure [41]. EC measurements were conducted under ambient N_2 (1 atm) using a glass cell that included a platinum counter electrode and a reversible hydrogen electrode (RHE). All potentials presented in this paper are stated with respect to RHE. CV curves of the UHV-prepared sandwich surfaces were recorded in N_2-purged 0.1 M $HClO_4$ (Merck, Suprapur) without sample disk rotation after an EC surface cleaning procedure of the type described by Marković et al. was performed [31]. After at least 8 cycles of CV measurements, linear sweep voltammetry (LSV) curves were collected in O_2-saturated 0.1 M $HClO_4$ at various disk rotation rates. The ORR activity of the Pt/Ni/Pt structures were evaluated from the kinetically controlled current densities (j_k) at 0.9 V, which were estimated from the Koutecky–Levich plots [31].

3. Results and discussion

CV curves for a series of UHV-prepared Pt/Ni/Pt(1 1 1) and Pt/Ni/Pt(1 1 0) atomic sandwich structures are summarized in Figs. 1(a) and (b). Hydrogen adsorption and desorption characteristics are known to be sensitive to the surface atomic arrangements of Pt [45]. In fact, the curve for the clean Pt(1 1 1) (dotted line) (a) is characterized by symmetrical features located at 0.05–0.35 V (hydrogen-related peaks) and at 0.8 V (hydroxyl-related peaks, forming a so-called "butterfly") [32]. In contrast, the CV curve of clean Pt(1 1 0) (dash-dotted) exhibits a remarkable redox feature due to hydrogen adsorption and desorption at 0.13 V and the curve corresponds well to the previously published CV curve of clean Pt(1 1 0) [31].

The CV curves of a series of Pt/Ni/Pt(1 1 1) structures (a) exhibit systematic changes in their above-mentioned hydrogen- and hydroxyl-related regions. The symmetrical hydrogen adsorption and desorption regions (0.05–0.35 V) changed markedly in the case of $Pt_{1ML}/Ni_{1ML}/Pt(1\,1\,1)$ (red): hydrogen charges decrease from 0.2 to 0.35 V, and the redox peaks at approximately 0.13 V emerge. With respect to the CVs of $Pt_{2ML}/Ni_{1ML}/Pt(1\,1\,1)$ and $Pt_{2ML}/Ni_{2ML}/Pt(1\,1\,1)$, the redox features at 0.13 V become uncertain. The shapes of CV curves were stable during the CV measurements in comparison to that for the $Pt_{1ML}/Ni_{1ML}/Pt(1\,1\,1)$. The Pt–M bimetallic

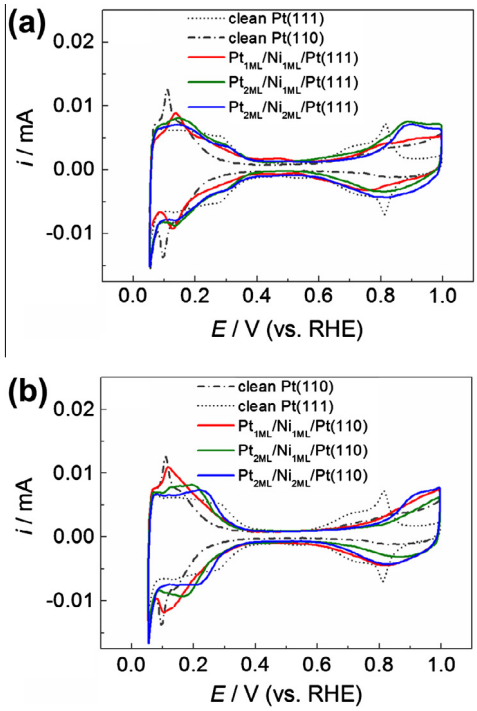

Fig. 1. (a) CV curves for $Pt_{1ML}/Ni_{1ML}/Pt(1\,1\,1)$ (red line), $Pt_{2ML}/Ni_{1ML}/Pt(1\,1\,1)$ (green), and $Pt_{2ML}/Ni_{2ML}/Pt(1\,1\,1)$ (blue) structures recorded in N_2-purged 0.1 M $HClO_4$ (sweep rate: 50 mV/s); the curves for clean Pt(1 1 1) (black dotted) and (1 1 0) (black dash-dotted) are also presented as references. (b) CV curves for $Pt_{1ML}/Ni_{1ML}/Pt(110)$ (red), $Pt_{2ML}/Ni_{1ML}/Pt(1\,1\,0)$ (green), and $Pt_{2ML}/Ni_{2ML}/Pt(1\,1\,0)$ (blue) structures. (For interpretation of the references to color in this figure legend, the reader is referred to the web version of this article.)